RESEARCH PAPER

Epigenetics 9:11, 1461–1472; November 2014; © 2014 Taylor & Francis Group, LLC

TGF-β induces global changes in DNA methylation during the epithelial-to-mesenchymal transition in ovarian cancer cells

Horacio Cardenas[1], Edyta Vieth[1], Jiyoon Lee[1], Mathew Segar[2], Yunlong Liu[1,2,3,4], Kenneth P Nephew[3,5,6,7,8,*], and Daniela Matei[1,3,8,9,10,*]

[1]Department of Medicine; Indiana University School of Medicine; Indianapolis, IN USA; [2]Center for Computational Biology and Bioinformatics; Indianapolis, IN USA; [3]Indiana University; Melvin and Bren Simon Cancer Center; Indianapolis, IN USA; [4]Department of Medical and Molecular Genetics; Indiana University School of Medicine; Indianapolis, IN USA; [5]Department of Cellular and Integrative Physiology; Indiana University School of Medicine; Indianapolis, IN USA; [6]Molecular and Cellular Biochemistry Department; Indiana University; Bloomington, IN USA; [7]Medical Sciences Program; Indiana University School of Medicine; Bloomington, IN USA; [8]Department of Obstetrics and Gynecology; Indiana University School of Medicine; Indianapolis, IN USA; [9]VA Roudebush Hospital; Indianapolis, IN USA; [10]Department of Biochemistry and Molecular Biology; Indiana University School of Medicine; Indianapolis, IN USA

Keywords: DNA methylation, EMT, ovarian cancer, SGI-110, TGF-β

Abbreviations: 15 DNMTI, DNMT inhibitor, CGI, CpG island, DNMT, DNA methyltransferase, EMT, epithelial-to-mesenchymal transition, HMA, hypomethylating agent, IPA, Ingenuity pathway analysis, mRNA, messenger ribonucleic acid, PCA, principal component analysis, TGF-b, transforming growth factor b, TSS, transcription start site.

A key step in the process of metastasis is the epithelial-to-mesenchymal transition (EMT). We hypothesized that epigenetic mechanisms play a key role in EMT and to test this hypothesis we analyzed global and gene-specific changes in DNA methylation during TGF-β-induced EMT in ovarian cancer cells. Epigenetic profiling using the Infinium HumanMethylation450 BeadChip (HM450) revealed extensive ($P < 0.01$) methylation changes after TGF-β stimulation (468 and 390 CpG sites altered at 48 and 120 h post cytokine treatment, respectively). The majority of gene-specific TGF-β-induced methylation changes occurred in CpG islands located in or near promoters (193 and 494 genes hypermethylated at 48 and 120 h after TGF-β stimulation, respectively). Furthermore, methylation changes were sustained for the duration of TGF-β treatment and reversible after the cytokine removal. Pathway analysis of the hypermethylated loci identified functional networks strongly associated with EMT and cancer progression, including cellular movement, cell cycle, organ morphology, cellular development, and cell death and survival. Altered methylation and corresponding expression of specific genes during TGF-β-induced EMT included *CDH1* (E-cadherin) and *COL1A1* (collagen 1A1). Furthermore, TGF-β induced both expression and activity of DNA methyltransferases (DNMT) -1, -3A, and -3B, and treatment with the DNMT inhibitor SGI-110 prevented TGF-β-induced EMT. These results demonstrate that dynamic changes in the DNA methylome are implicated in TGF-β-induced EMT and metastasis. We suggest that targeting DNMTs may inhibit this process by reversing the EMT genes silenced by DNA methylation in cancer.

Introduction

DNA methylation at carbon 5 of cytosines (5-methylcytosine or 5 mC) and typically in a CpG context plays an important role regulating gene transcription and represents the best characterized epigenetic modification. CpG methylation is mediated by DNA methyltransferases (DNMTs), primarily DNMT-1 (regulates predominantly maintenance (one strand) methylation) and DNMT-3A and -3B (catalyze *de novo* methylation).[1,2] More recently, regulation of DNA methylation has been shown to also involve demethylases that remove the cytosine methyl group through hydroxylation or glycosylation.[3,4] For instance the 10-11 translocation (Tet) proteins catalyze the conversion of 5mC to 5-hydroxymethylcytosine (5hmC) and have been implicated in the maintenance of embryonic stem cells.[5] Both increased methylation leading to silencing of tumor suppressor genes and hypomethylation, linked to genomic instability, have been documented in the context of cancer genomes and strongly implicated in cancer initiation, as well as in tumor progression.[2]

The process of epithelial-to-mesenchymal transition (EMT) is critical to initiation of metastasis in solid tumors. EMT is characterized by the break-down of cell junctions and loss of cell polarity, rendering epithelial cells motile and invasive.[6] An important regulatory phase during EMT is the loss of type I cadherins which maintain stable cell-cell contacts.[7] Downregulation of E-cadherin (*CDH1* gene) causes a mesenchymal phenotype,[6,8] and

*Correspondence to: Daniela E Matei; Email: dmatei@iupui.edu; Kenneth P Nephew; Email: knephew@indiana.edu
Submitted: 06/20/2014; Revised: 08/29/2014; Accepted: 09/22/2014
http://dx.doi.org/10.4161/15592294.2014.971608

is regulated by several well described transcriptional repressors, including *Slug*, *Snail, Twist, Zeb 1,2,* and *E47.*[9] However, in addition to standard transcriptional regulation, the *CDH1* promoter has been reported to be methylated,[10] and induction of EMT has been shown to repress *CDH1* expression through epigenetic silencing in breast cancer cells.[11] Additionally, other genes implicated in EMT, such as *Snail*, have recently been shown to be modulated epigenetically.[12-14] Whether and how global and gene specific changes in DNA methylation contribute to the EMT process is currently unknown.

Transforming growth factor-β (TGF-β) plays a complex role in cancer, having both tumor suppressor and oncogenic activities.[19] Signaling from TGF-β has been shown by us and others to be functional in ovarian cancer,[15-17] acting as a potent inducer of ovarian cancer invasiveness by regulating proteins involved in metastasis[18,19] and contributing to EMT and increased metastasis.[20] TGF-β ligands and type I and type II TGF-β receptors are expressed in over 50% of ovarian tumors,[21-23] and TGF-β is abundantly secreted in the peritoneal environment by both cancer and stromal cells.[15] Although a known inhibitor of epithelial cell proliferation,[24] TGF-β growth inhibitory signals have been shown to be blocked in malignancy, resulting in neoplastic epithelial cell insensitivity to TGF-β. This loss of TGF-β-induced inhibition of epithelial cell proliferation has been attributed to inactivating mutations in TGF-β receptor I and II, which have been detected in ovarian cancer,[25,26] as well as to alterations of cell signaling downstream of SMADs.[15] While TGF-β-induced EMT is a well characterized model system, epigenetic changes occurring during this process have not been well defined.

To study global DNA methylation during EMT, we conducted a time course study using TGF-β stimulation of ovarian cancer cells. We demonstrate for the first time that the cytokine induces global changes in the ovarian cancer DNA methylome, resulting in hypermethylation of key genes and alterations in several oncogenic pathways. TGF-β-induced changes in promoter methylation and expression of specific genes, including *CDH1* and *COL1A1* (*collagen 1A1*), were validated in ovarian cancer cell lines. The effects of TGF-β were mediated primarily through increased expression and activity of DNMTs and reversible upon TGF-β withdrawal. The novel DNMT inhibitor SGI-110 blocked EMT gene-specific changes and reversed the TGF-β-induced mesenchymal phenotype. In all, our data support that aside from its well described effects on gene transcription, TGF-β alters the activity of DNMTs, resulting in global and gene specific DNA methylation gains and losses that contribute to its oncogenic activities in ovarian and perhaps other cancers.

Results

TGF-β induces global changes in the DNA methylome and EMT in SKOV3 cells

To investigate changes in DNA methylation during TGF-β-induced EMT, SKOV3 cells were treated with TGF-β1 for up to 5 d. Distinct morphological changes were observed, as cells changed from the cobblestone appearance characteristic of epithelial cells (**Fig. 1A**, panels I-III) to the fusiform shape indicative of a mesenchymal phenotype occurring as part of EMT (**Fig. 1A**, panels IV & V). These morphological changes were accompanied by decreased expression of the epithelial marker, E-cadherin, and increased expression of the mesenchymal marker, vimentin, as assessed by western blotting (**Fig. 1A**). Morphological changes were partially reversible after TGF-β removal (**Fig. 1A**, panel VI).

Genome-scale DNA methylation was measured using the HM450 BeadChip platform after 48 h and 120 h of TGF-β stimulation, and 48 h after removal of the cytokine (120 h + 48 h off). Methylation was altered at >400 of CpGs ($P < 0.01$ and FDR < 0.05), of which approximately a third remained stably altered for the duration of treatment (**Table 1**). Similarly, TGF-β increased the average methylation values of ~500 CGIs located in or near gene promoters, defined as regions encompassing −2000 to +500 nucleotides relative to the TSS (**Table 2**). The majority of changes occurring at 48 h were sustained for the treatment duration. Importantly, after TGF-β withdrawal, gene methylation changes returned to control levels (**Tables 1 and 2**), suggesting that the continuous presence of the cytokine was necessary to maintain de novo methylation patterns generated during EMT. Reversal of DNA methylation patterns after cytokine removal was also supported by the similarity in methylation patterns of the control (untreated) and the TGF-β treated and "wash-off" (120 h + 48 h off) groups (unsupervised hierarchical clustering analysis, **Figure 1B**; principal component analysis (PCA), **Fig. 1C**).

Although treatment with TGF-β induced DNA methylation changes throughout the SKOV3 epigenome, increased DNA methylation levels represented the majority of significant changes (**Tables 1 and 2**). This global effect was also reflected in an overall increase of average β-values of all CpG sites at 48 and 120 h (**Fig. 1D**). Consistently, methylation of long interspersed element-1 (LINE-1), a reliable indicator of global DNA methylation[27-29] was also increased by TGF-β at the same time points during induction of EMT (**Fig. 1E**).

To investigate potential gene interactions among putative transcripts regulated by TGF-β-induced CGI hypermethylation, IPA bioinformatics tools were used. Significantly associated network functions (**Table 3**) and molecular and cellular functions (**Table 4**) were identified. IPA analysis further revealed many genes associated with biological pathways relevant to cancer. For example, **Figure 1F** shows a network containing 22 genes associated with CGI hypermethylation linked with at least one of the following pathways: TGF-β, PI3K, MAPK, NFκB, VEGF, or Akt. The top hypermethylated genes in the networks were: *GPR135, ZC3HAV1L, QRICH2, CLDN3, TPTE2, SPAG6, RNF212, CYYR1, ASF1A, CDH7, MTNR1B, LHX8, GRIN3B, CT47B1, SLC12A4, GDNF, C1orf65*; those with decreased methylation were *ARL4D and TGFB1* (**Supplementary Table S1**). The top molecular and cellular functions associated with significant changes in promoter CGI methylation identified by IPA included: cell-cell signaling and interaction, cell cycle, cellular

movement, cell death and survival, and cell morphology (**Table 4**).

TGF-β regulates DNMT expression and activity

To investigate the potential mechanisms underlying TGF-β-induced changes in DNA methylation, we examined expression levels of DNA methyltransferases (DNMT-1, -3A, and -3B) and demethylases (TET-1 and -2), and effects of TGF-β on total DNMT activity. At the mRNA level, increased *DNMT-1, -3A* and *-3B* expression was observed by 12 h after TGF-β stimulation (**Fig. 2A**). Prolonged stimulation with TGF-β (48 and 120 h) was associated with increased *DNMT-1, -3A* and *-3B* mRNA expression levels (**Fig. 2B**). DNMT-1 and -3B nuclear protein levels were also increased after 24 and 48 h of TGF-β treatment (**Fig. 2C**). DNMT-3A protein was not detectable in this cell line (not shown). Increased *DNMT-1, -3A* and *-3B* mRNA expression levels in response to TGF-β were also noted in Hey C2 cells (**Supplementary Fig. S1**) and increased DNMT-3B protein levels were recorded in HeyC2 IGROV1 and OVCAR3 ovarian cancer cells and in the immortalized ovarian surface epithelial (IOSE) cells (**Supplementary Fig. S2**). In contrast, DNMT1 expression levels remained unchanged after TGF-β treatment in these cells (not shown). Furthermore, the total DNMT activity measured in nuclear extracts of SKOV3 cells was increased after 48 h of TGF-β treatment (**Fig. 2D**), indicating elevated methyltransferase functional activity. Interestingly, by 48 h after TGF-β removal, DNMT activity returned to baseline levels, consistent with the observed reversal of DNA methylation patterns (**Fig. 1B–E**). We also examined the effects of TGF-β on expression of 2 proposed DNA demethylases, TET-1 and

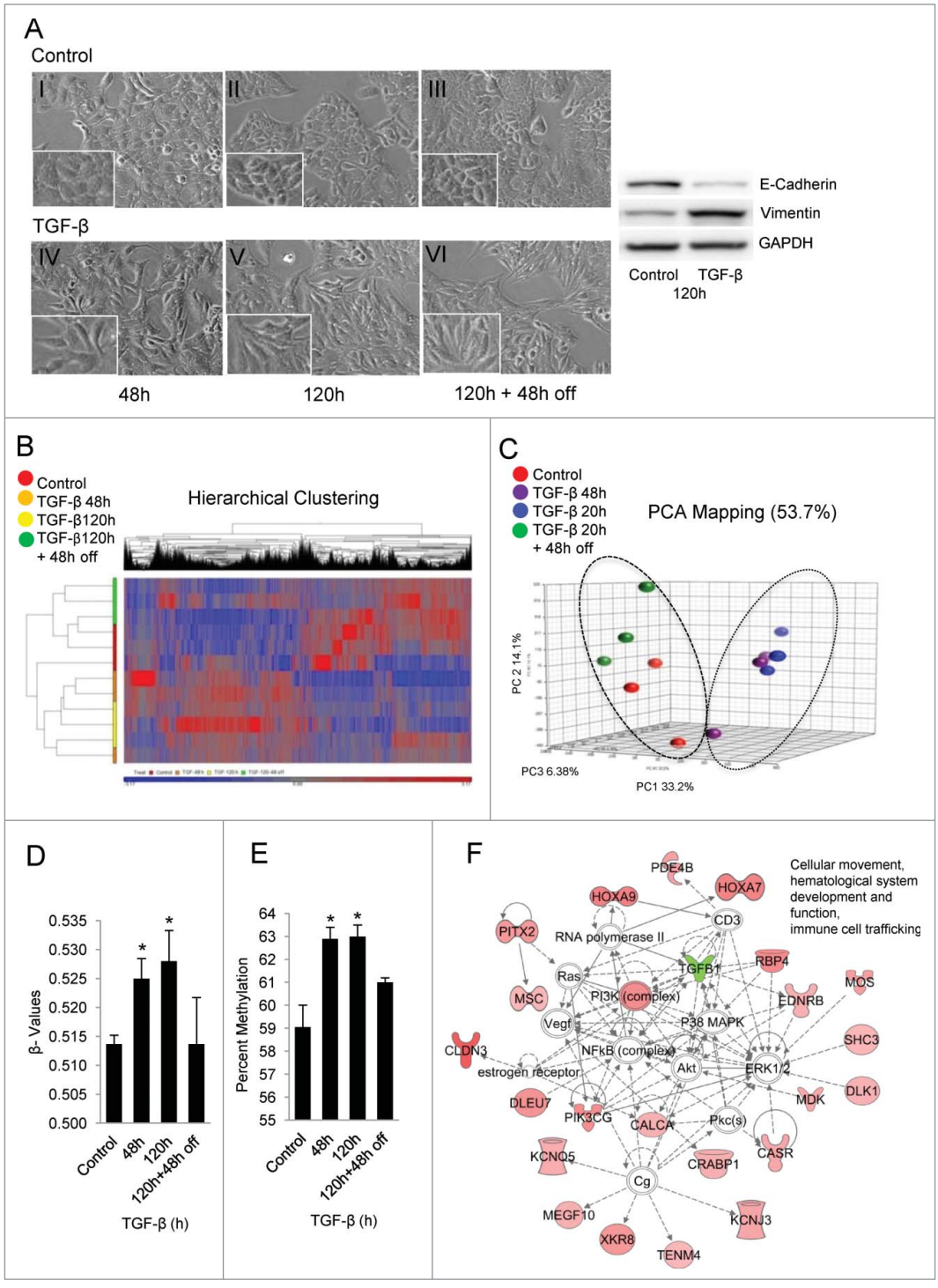

Figure 1. For figure legend, see page 1464.

Table 1 Numbers of CpG sites associated with significant changes in methylation during TGF-β -induced EMT in SKOV3 cells[a]

	Increased Methylation		Decreased Methylation	
Comparisons	**Numbers**	**Δβ Range[b]**	**Numbers**	**Δβ Range[b]**
48 h vs. Control	351	0.007–0.168	117	0.010–0.151
120 h vs. Control	344	0.007–0.145	46	0.009–0.130
120 h + 48 h off vs. Control	35	0.026–0.297	45	0.020–0.317
Common changes at 48 and 120 h	130	-	30	-

[a]Cells were treated with TGF-β (5 ng/ml) for 48 h, 120 h, or 120 h followed by TGF-β removal for 48 h (120 h + 48 h off). Significant changes: $P < 0.01$ (ANOVA) and FDR < 0.05.
[b]Δβ = Difference in average β-values between treatments per CpG site.

-2,[5,30] but no changes in TET1 and TET-2 mRNA expression levels were observed after 24 and 120 h of TGF-β treatment (**Supplementary Fig. S3**; $P > 0.05$). Collectively, these results support a role of TGF-β in the regulation of DNA methylation through direct effects on DNMTs expression and activity.

TGF-β-induced changes in DNA methylation are associated with gene expression changes

Functional relevance of the DNA methylation changes induced by TGF-β was assessed by examining expression of specific genes displaying altered methylation and relation with EMT,[31] including *COL1A1*, an EMT-associated gene known to be upregulated by TGF-β and which contains promoter CpGs, but lacks a promoter SMAD binding site. To verify that the effects of TGF-β were in fact mediated through DNA methylation, we used SGI-110, a novel DNMT1 inhibitor.[32,33] The mRNA expression levels of *COL1A1* were increased by TGF-β at 48 and 120 h and also upregulated by treatment with SGI-110 alone (**Fig. 3A**) suggesting promoter demethylation contributes to *COL1A1* transcriptional regulation. Combined treatment with TGF-β and SGI-110 further enhanced *COL1A1* expression (**Fig. 3A**), supporting the notion that the effects of TGF-β are mediated through changes in promoter methylation. In contrast, the expression of *COL5A1* (*collagen 5A1*) was induced by TGF-β, but was not altered by SGI-110 alone or in combination with TGF-β (**Fig. 3B**), suggesting that the effects of the cytokine on *COL5A1* expression were not mediated through DNA methylation. Similar effects of TGF-β and SGI-110 on *COL1A1* and *COL5A1* mRNA expression levels were observed in additional ovarian cancer cell lines (Hey and HeyC2, **Fig. 3C**).

To further examine the mechanism of TGF-β activity on *COL1A1* promoter methylation and transcriptional reactivation, we searched for potential transcription factor binding sites (TFBS) around the *COL1A1* TSS using PROMO software (http://alggen.lsi.upc.es/cgi-bin/promo_v3). A binding site for specificity protein 1 (SP1) is present at position −88 to −79 (NCBI RefSeq: NG_007400.1 and Transcription Regulatory Element Database # 18363) relative to the *COL1A1* TSS (**Fig. 3D**). A previous report demonstrated that by recruiting the active unit of the NF-κB complex RelA to this promoter region, SP1 repressed *COL1A1* expression.[34] Pyrosequencing analysis of the 3 CpG sites in the *COL1A1* promoter confirmed that TGF-β treatment resulted in increased ($P < 0.05$) methylation levels of the SP1 binding region CpG sites (**Fig. 3E**). Based on these observations, we speculated that methylation of these CpG sites may interfere with binding of RelA and SP1 transcription factors to the *COL1A1* promoter. To demonstrate that RelA plays a role in the TGF-β mediated regulation of *COL1A1,* we used siRNA to knockdown *RelA* (**Fig. 3F**, left) and subsequently measured response to TGF-β. Knockdown of *RelA* augmented TGF-β-mediated *COL1A1* induction (**Fig. 3F**, right), suggesting that RelA inhibits *COL1A1* transcription in response to this cytokine. We propose that hypermethylation of these specific CpG sites induced by TGF-β-regulated DNMTs makes this promoter region resistant to the inhibitory effects of RelA and SP1 and allows for induction of *COL1A1* expression, illustrating for the

Figure 1 (See previous page). TGF-β induces changes in DNA methylation during EMT in ovarian cancer cells. (**A**) Phase contrast microscopy identifies morphological changes induced in SKOV3 cells by TGF-β (5 ng/ml) at 48, 120, and 48 h after removal of TGF-β (magnification 100×, panels; 200×, insets). Western blotting for E-cadherin and vimentin in SKOV3 cells treated with TGF-β for 120 h (right panel). (**B**) Unsupervised hierarchical clustering displays differential DNA methylation profiles of SKOV3 cells treated with vehicle, TGF-β for 48 and 120 h, or 48 h after removal of TGF-β (n = 3 replicates per group; each group is color coded). Rows represent individual samples and columns represent CpG sites β-values. A visual dual color code is utilized with red and blue indicating high and low expression levels, respectively. The scale of color saturation reflects β-values for individual CpG sites. (**C**) Unsupervised sample classification based on principal component analysis of DNA methylation profiles of SKOV3 cells treated with TGF-β for the indicated time points (3 replicates per group). Samples with similar profiles cluster together. (**D**) Average β-values for all CpG sites in SKOV3 cells treated with TGF-β (5 ng/ml) for 48, 120, and 48 h after removal of TGF-ß. (**E**) Effects of TGF-β on average percent methylation of 4 CpG sites of the *LINE-1* sequence at the indicated timepoints were determined by pyrosequencing. Bars represent means of 3 replicates ± SE. * denotes $P < 0.05$. (**F**) Gene networks were ranked by log *P*-values and compared TGF-β treated versus control SKOV3 cells. Analysis within the top ranked networks (log *P*-value > 25) displays interconnected genes as nodes. Genes are colored according to expression levels, red symbols corresponding to up-regulated genes and green symbols indicating downregulation. Dashed lines between nodes show indirect interactions; continuous lines indicate direct interactions.

Table 2 Numbers of CpG islands associated with significant changes in methylation during TGF-β-induced EMT in SKOV3 cells[a]

	Increased Methylation		Decreased Methylation	
Comparisons	**Numbers**	**Δβ Range[b]**	**Numbers**	**Δβ Range[b]**
48h vs. Control	193	0.008–0.088	2	0.036–0.049
120h vs. Control	494	0.007–0.085	1	0.042
120h + 48h off vs. Control	0	—	3	0.028–0.043
Common changes at 48 and 120h	138	—	0	—

[a]Cells were treated with TGF-β (5 ng/ml) for 48 h, 120 h, or 120 h followed by TGF-β removal for 48 h (120 h + 48 h off). Significant changes: $P < 0.01$ (ANOVA) and FDR < 0.05.
[b]Δβ = Difference in average β-values between treatments per CpG island.

first time a SMAD-independent effect of TGF-β on gene expression.

SGI-110-induced global DNA hypomethylation represses EMT

To demonstrate the functional significance of DNA methylation to EMT regulation, we determined the effects of the hypomethylating agent (HMA) SGI-110 on TGF-β-stimulated ovarian cancer cells. As expected, TGF-β induced EMT (**Fig. 4A**, panels I vs. II), while the epithelial characteristics of these cells were maintained by concomitant treatment with SGI-110 (**Fig. 4A**, panel III), indicating that inhibition of methylation prevents TGF-β-induced EMT (**Fig. 4A**). No change in the morphology of cells treated with HMA alone was observed (**Fig. 4A**, panel I vs. IV). To further quantify the effects of SGI-110 on known markers of EMT, expression of *CDH1* and *FN1* (fibronectin 1) was examined. Treatment with SGI-110 increased *CDH1* mRNA levels (**Fig. 4B**), suggesting that promoter methylation regulated expression of this epithelial marker and prevented TGF-β-induced E-cadherin downregulation. In contrast, no change in *FN1* mRNA expression level was observed after HMA treatment (**Fig. 4B**), suggesting that this mesenchymal marker is not regulated by promoter methylation. Pyrosequencing analysis confirmed that SGI-110 prevented TGF-β-induced *CDH1* promoter methylation (**Fig. 4C**).

To analyze the global effects of SGI-110 on TGF-β-induced EMT, a pathway specific quantitative RT-PCR array was used to examine 84 genes known to be associated with EMT. Upregulation (>2-fold increase) of a significant number of genes (23 out of 84) was observed in cells treated with SGI-110 (**Table 5**). Furthermore, SGI-110 induced marked (>50 fold) upregulation of several genes, including *COL1A2, COL3A1, IGFBP4, KRT14,* and *TGFB2* (**Table 5**), suggesting a prominent role for DNA methylation in expression of these genes.

Analysis of transcripts whose regulation by TGF-β was prevented by SGI-110, point to genes potentially regulated by TGF-β through DNA methylation changes (**Table 5**). Among those, the array confirmed that SGI-110 blocked TGF-β-induced downregulation of *CDH1*. In addition, upregulation of *ZEB2*, a known *CDH1* transcriptional repressor and inducible by TGF-β, was partially suppressed by the combined treatment of TGF-β and SGI-110. Induction of *ZEB1* and *2* and *SNAIL1* expression levels by TGF-β and by treatment with SGI-110 were confirmed by qRT-PCR (**Fig. 4D**), indicating that epigenetic modulation of key transcription factors represents a potential mechanism of EMT regulation. Based on these results, we suggest that TGF-β-induced changes in DNA methylation alter transcription of critical genes that significantly contribute to regulatory mechanisms controlling EMT.

Table 3 Top IPA identified networks including genes displaying significant changes in promoter associated CpG islands methylation during TGF-β-induced EMT

Associated Network Functions	Score
Digestive system development and function, organ morphology, organismal development.	54
Cellular movement, hematological system development and function, immune cell trafficking.	46
Respiratory system development and function, embryonic development, organ development.	28
Embryonic development, organismal development, cellular development	24
Behavior, cell death and survival, nervous system development and function	20

Discussion

Our study provides important new information on the role of DNA methylation and EMT induction in ovarian cancer cells. Initiation of the EMT program imparts to cancer cells the ability to invade and disseminate,[35] and completion of EMT has been linked to the generation of cells with stem-like properties.[36] This theory may explain, at least in part, how metastatic cells can form neoplastic colonies at distant sites and allow metastasis to be

Table 4 Top IPA identified molecular and cellular functions including genes showing significant changes in promoter associated CpG islands methylation during TGF-β-induced EMT

Molecular and Cellular Functions	*P*-values	Numbers of Molecules
Cell-cell signaling and interaction	6.04E-08 – 2.85E-02	24
Cell cycle	7.25E-05 – 1.48E-02	6
Cellular movement	3.06E-04 – 2.85E-02	22
Cell death and survival	3.06E-04 – 2.85E-02	10
Cell morphology	5.08E-04 – 2.85E-02	19

established. The initiation and maintenance of the EMT process depends on signals provided by the tumor microenvironment, such as TGF-β, PDGFs, and other growth factors or cytokines that induce malignant epithelial cells to lose their epithelial characteristics and acquire invasive traits.[35] It is accepted that a variety of transitory and plastic states ranging between pure epithelial and pure mesenchymal phenotypes may co-exist in a highly heterogeneous "mix" during the process. The EMT program is tightly regulated by transcriptional activators and repressors engaged by the paracrine and autocrine cues from the tumor microenvironment. Here we provide the first evidence that activity of EMT transcriptional regulators in ovarian cancer cells is modulated in part by the methylation state of the DNA.

Recent reports have begun to document the involvement of epigenetic mechanisms during the EMT program, particularly of histone and chromatin modifications. For instance the polycomb repressor group 2 (PRC2), which modulates trimethylation of K27 on histone H3 (H3K27me3), has been shown to repress *CDH1*.[37,38] The lysine specific demethylase LSD1, which removes a methyl group from the H3K4me3 transcription active mark, has been shown to interact with, and be required for, Snail-1-induced *CDH1* repression.[12] Epigenetic reprogramming dependent on LSD1 and involving chromatin reconfiguration, but not changes in DNA methylation, has also been demonstrated in hepatocytes undergoing EMT.[37] Conversion of the bivalent chromatin configuration bearing both repressive H3K27me3 and active H3K4me3 marks at the *ZEB1* promoter, to an active configuration that lacks the H3K27me3 mark, allows increased

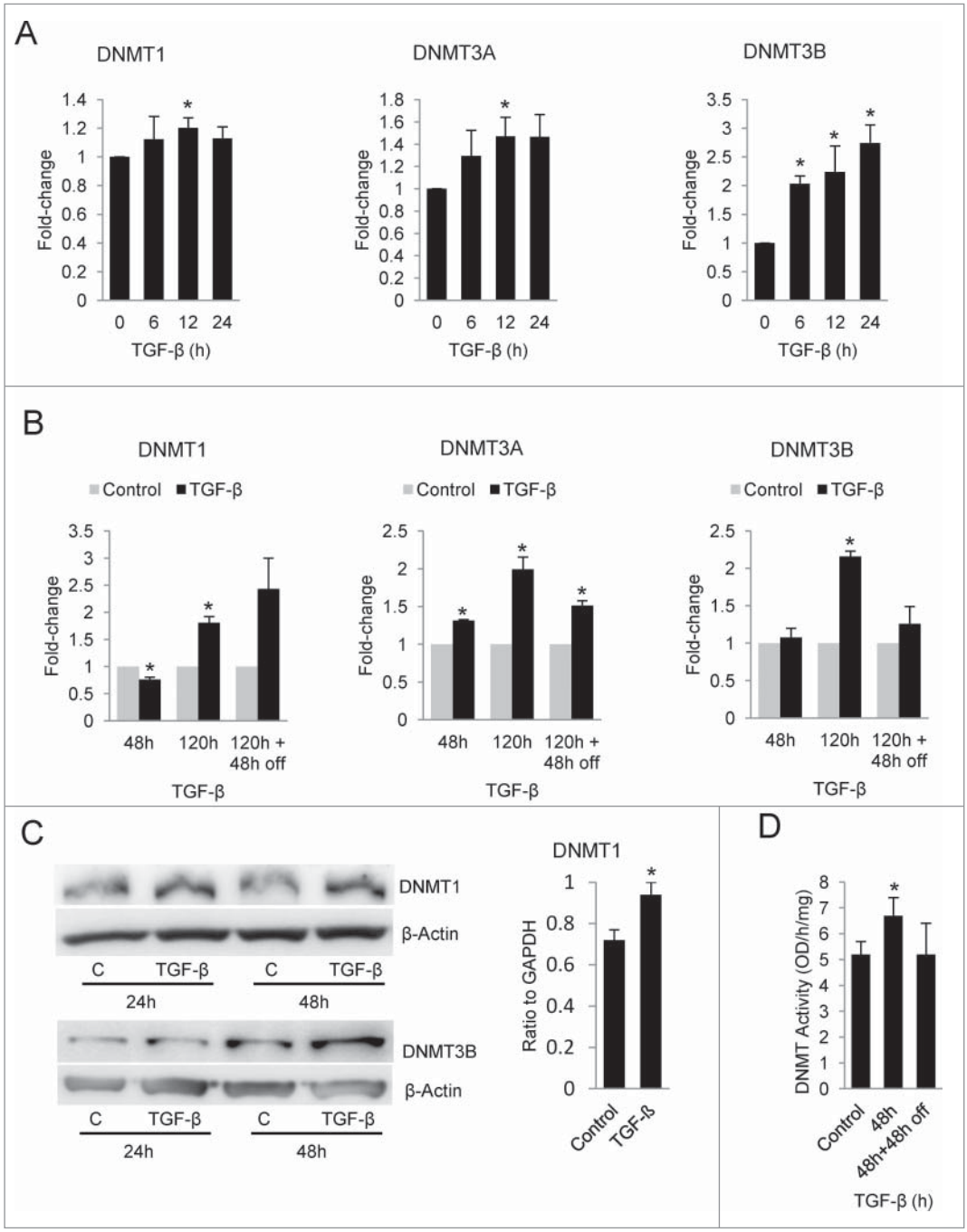

Figure 2. TGF-β regulates expression and activity of DNMTs in SKOV3 cells. (**A–B**) Real-time RT-PCR measures mRNA expression levels of DNMT-1, -3A, and -3B in SKOV3 cells treated with TGF-β (5 ng/mL) for different periods of time, as indicated. Data are shown as means ± SE of 3 replicate measurements. (**C**) Western blotting for DNMT-1 and -3B in nuclear lysates of SKOV3 cells treated with TGF-β for 24 and 48 h (left panel) and corresponding densitometric analysis for DNMT1 (n = 4 replicates, right panel). (**D**) DNMT activity measured in nuclear lysates of SKOV3 cells treated with TGF-β (5 ng/mL) for 48 h and allowed to recover for 48 h after TGF-β removal (n = 4 replicates). Bars represent means ± SE. * denotes statistical significance ($P < 0.05$) vs. 0 h.

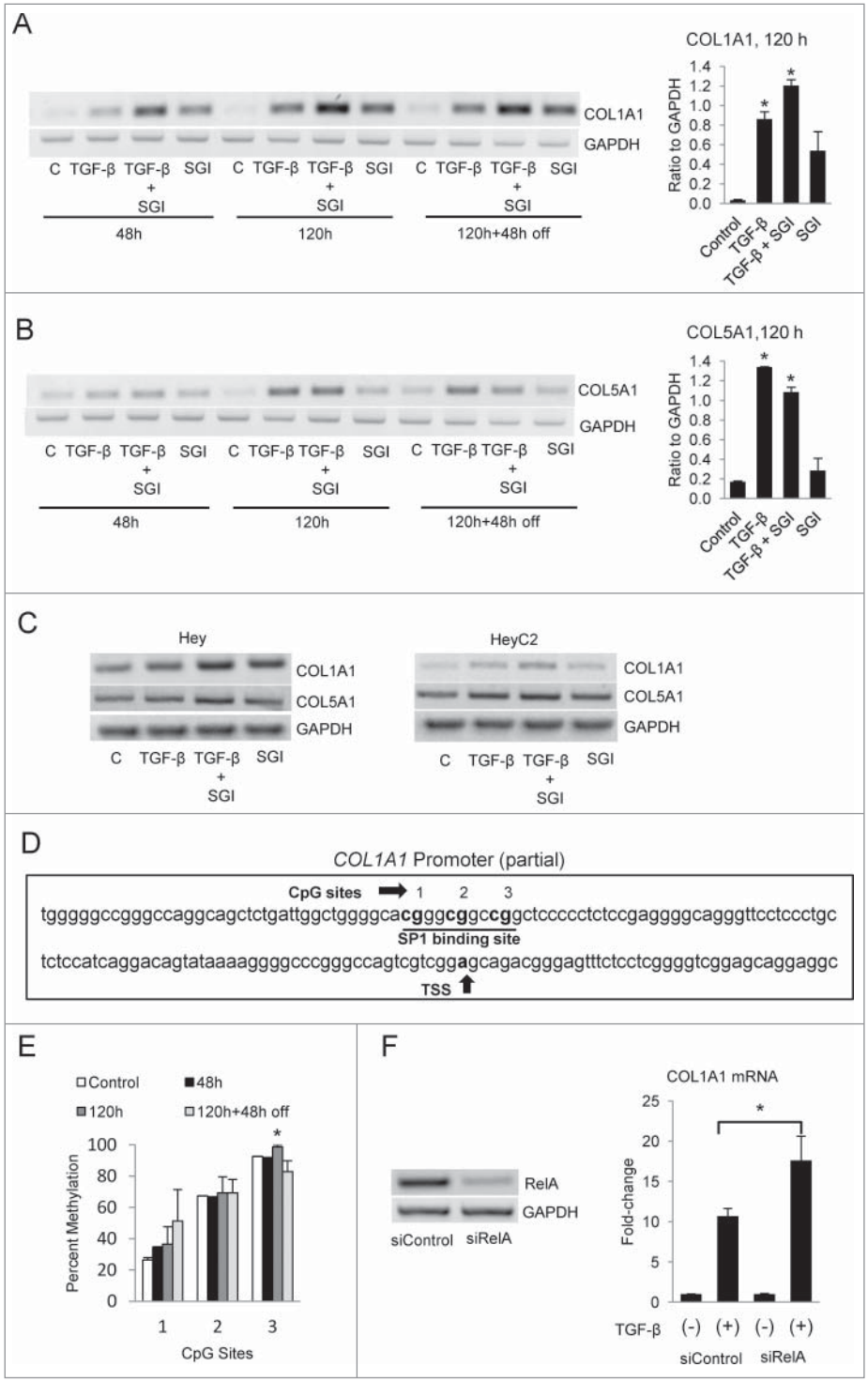

Figure 3. Correlation between DNA methylation and gene expression during TGF-β -induced EMT. A–B. Semiquantitative RT-PCR (left panels) and densitometric analysis (right panels) measures *mRNA* expression levels of *COL1A1* (**A**) *and COL5A1* (**B**) in SKOV3 cells treated with TGF-β (5 ng/ml), SGI-110 (5 μM), or the combination for 48 h, 120 h and allowed to recover for 48 h after TGF-β removal. Bars in right panels represent means of 3 replicates ± SE. * denotes $P < 0.05$ compared to control. (**C**) Semiquantitative RT-PCR measures *mRNA* expression levels of *COL1A1 and COL5A1* in Hey (left) and HeyC2 cells (right) treated with TGF-β (5 ng/ml), SGI-110 (5 μM), or the combination for 48 h. (**D**) Schematic representation of the *COL1A1* promoter illustrates presence of 3 CpG sites located in the proximity of a known SP1 binding site. (**E**) Effects of TGF-β on percent methylation of the 3 CpG sites in the *COL1A1* promoter at the indicated timepoints (48 h, 120 h, and 48 h recovery) were determined by pyrosequencing. Bars represent means of 3 replicates ± SE. * denotes $P < 0.05$ compared to control. (**F**) Semiquantitative RT-PCR measures *RelA mRNA* expression levels in SKOV3 cells transfected with scrambled siRNA (control) or siRNA targeting *RelA* (left panel). Real-time PCR measures *COL1A1* mRNA expression levels in SKOV3 cells transfected with scrambled siRNA (control) or siRNA targeting *RelA* and treated with vehicle or with TGF-β (5 ng/ml) for 48 h (right panel). Bars represent means of 3 replicates ± SE. * denotes $P < 0.05$.

transcription of the well characterized EMT inducer Zeb1 and promotes transition of cancer non-stem cells into stem cells.[39] However, the involvement of DNA methylation in the induction and maintenance of a mesenchymal phenotype is much less well described.

Here we show that in ovarian cancer cells, stimulation with TGF-β induces global DNA hypermethylation, impacting transcription of EMT-associated genes, including the key epithelial marker *CDH1* and demonstrating the first "SMAD-independent" effect of TGF-β on gene expression. While the methylation changes observed were on average relatively modest (**Tables 1 and 2**), we demonstrate that some of these changes were functionally relevant, being associated with differential expression of specific genes (e.g., *CDH1* and *COL1A1)*. Interestingly, the increase in DNA methylation during EMT was reversible upon TGF-β withdrawal, coinciding with resumption of epithelial characteristics. While patterns of DNA methylation are considered to remain relatively stable overtime, variations in promoter methylation leading to gene silencing have been shown to occur in association with DNA repair[40] or in response to micro-environmental factors, such as increased reactive oxygen species during inflammation.[41] The observed effects of TGF-β on DNMTs expression level and methylation changes were more pronounced with prolonged exposure to the cytokine (120 h compared to 48 h), consistent with the concept

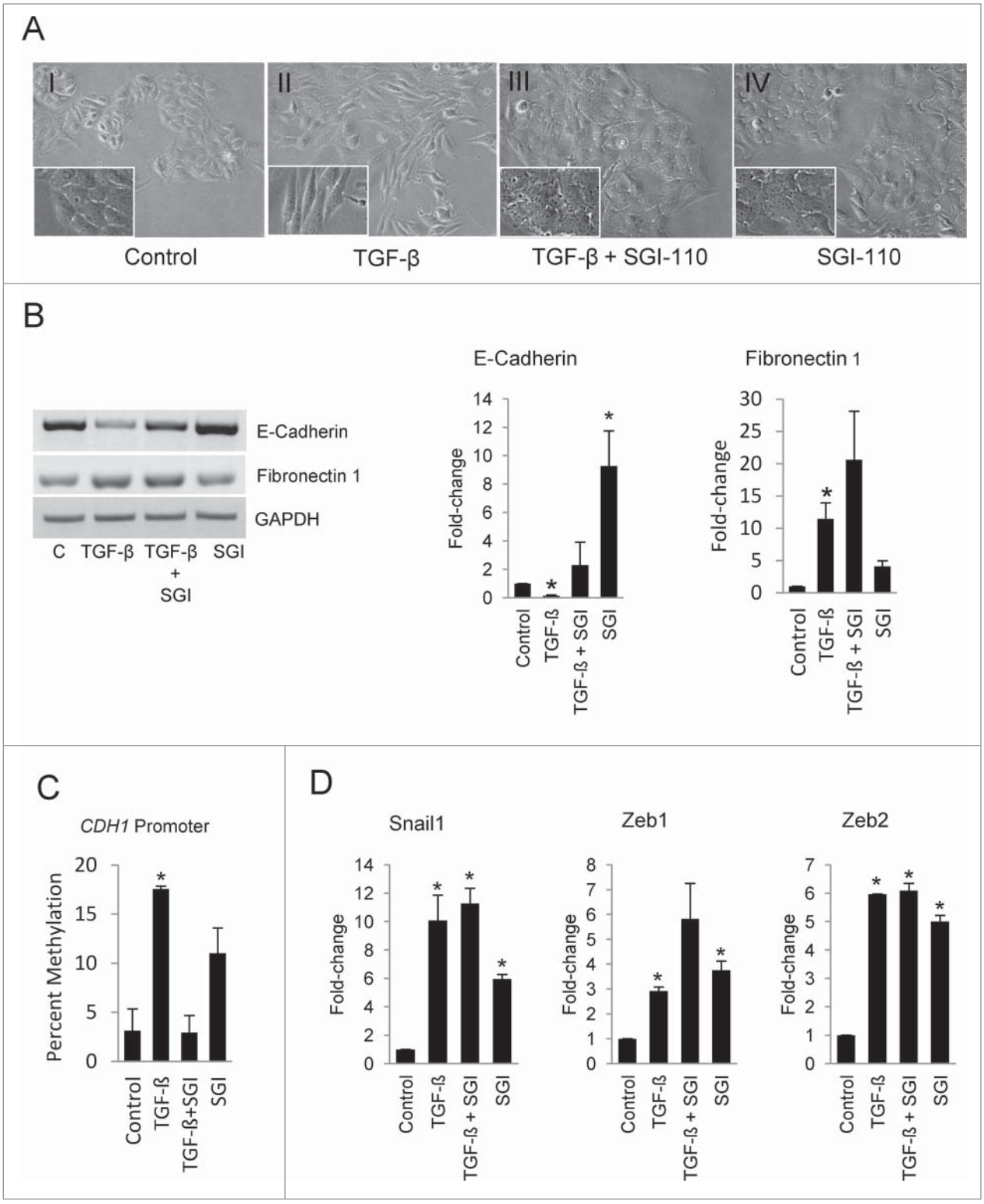

Figure 4. The DNMT inhibitor SGI-110 blocks TGF-β-induced EMT in SKOV3 cells. (**A**) Phase contrast microscopy identifies morphological changes induced in SKOV3 cells by TGF-β (5 ng/ml), SGI-110 (5 μM), or the combination (100× for panels and 200× magnification for insets, left panels). (**B**) Semi-quantitative (left panel) and real-time RT-PCR (right and middle panels) measures mRNA expression levels of *CDH1* (E-cadherin) and *FN1* (fibronectin) in SKOV3 cells treated with TGF-β (5 ng/ml), SGI-110 (5 μM), or the combination (n = 2 replicates). Bars represent means of 2 replicates ± SE. * denotes $P < 0.05$ compared to control. (**C**) Effects of TGF-β and SGI-110 on average methylation of CpG sites in the *CDH1* promoter were determined by pyrosequencing. Bars represent means of 3 replicates ± SE. * denotes $P < 0.05$ compared to control. (**D**) Real-time RT- PCR measures *mRNA* expression levels of the EMT transcriptional regulators (*Snail1, Zeb1,* and *Zeb2*) in SKOV3 cells treated with TGF-β (5 ng/ml), SGI-110 (5 μM), or the combination. Bars represent means of 3 replicates ± SE. * denotes $P < 0.05$ compared to control.

Table 5 Changes in EMT-associated gene expression induced by TGF-β and by the hypomethylating agent SGI-110 in SKOV3 cells[a]

	Fold Change Up or Down vs. Control		
Gene	**TGF-β**	**TGF-β+SGI-110**	**SGI-110**
BMP1	2.7	3.1	2.1
CDH1	−6.9	−1.5	5.5
COL1A2	12.2	355.5	196.8
COL3A1	2.0	187.7	63.0
COL5A2	2.2	4.0	3.2
ERBB3	−4.3	1.2	6.7
FGFBP1	−2.3	−4.1	−2.9
FOXC2	1.9	5.1	5.7
GSC	2.3	2.3	7.6
IGFBP4	−1.1	106.4	99.8
IL1RN	−2.1	1.2	6.7
KRT14	3.5	384.7	90.2
KRT7	1.5	1.5	−2.2
MMP2	11.6	10.3	2.2
MMP3	1.7	9.2	13.2
MMP9	−1.3	4.0	13.6
RGS2	1.5	3.6	3.4
SNAI1	6.3	10.8	4.9
SNAI3	−1.1	−1.9	−2.3
SPP1	−1.6	−2.7	−3.5
TCF4	4.9	16.1	8.9
TFPI2	3.0	4.6	2.2
TGFB2	3.9	86.9	86.5
WNT11	−1.1	1.6	2.6
WNT5A	4.2	3.5	2.7
WNT5B	−1.1	27.3	39.8
ZEB2	5.8	3.6	2.4

[a] Shown are genes with >2-fold change induced by SGI-110 relative to control.

that both maintenance and *de novo* methylation occur during DNA replication. Our findings are consistent with recent reports documenting increased DNA methylation in association with increased expression and activity of DNMTs in basal like breast cancers,[13,42] which have well-characterized EMT features.[43] Focal promoter hypermethylation and global genomic histone marks redistribution were also observed in a Twist-induced model of EMT in mammary cells.[44] Interestingly, the TGF-β pathway was identified as a potential predictor of response to DNMT inhibitors in a genomic analysis of tumor biopsies[45] collected from patients with recurrent ovarian cancer treated with decitabine in a clinical trial.[46]

The involvement of DNMT1 in TGF-β-induced DNA methylation is supported by the demonstration that SGI-110 prevented induction of EMT and silencing of *CDH1* and by the observations that the activity and nuclear distribution of DNMT1 increased after TGF-β stimulation. This represents the first report demonstrating that a DNMT inhibitor (DNMTI) blocks TGF-β-induced EMT, supporting the concept that agents in this class could have powerful "metastasis preventing" effects. The massive effects of the HMA alone on EMT-associated genes further highlight the significance of epigenetic regulation of this key neoplastic phenomenon. As cancer stem cells are known to harbor EMT characteristics, it could be postulated that epigenetic modulators like SGI-110 also block stem-like properties. Indeed, we and others have recently shown that low dose DNMTIs inhibits the survival and tumor initiating properties of cancer stem cells.[47]

Our study is limited by the evaluation of changes in global DNA methylation associated with EMT in a single cell line. SKOV3 cells were selected as the primary model for study, because they readily undergo EMT in response to the cytokine, compared to other ovarian cancer cells. The effects of TGF-β on DNMTs expression levels and on specific transcripts were validated in other cells (Hey, Hey C2). Another limitation of this study relates to the use of the Infinium HumanMethylation450 Bead Chip Arrays which has restricted quantitative capacity,[48] contributing to a higher false discovery rate and a lower sensitivity for detecting CpG island density compared to newer sequencing technologies.

In all, our findings strongly support the involvement of epigenetic reprogramming during EMT, converge with emerging literature using other cancer models, and provide new key information on the functions of DNA methylation during this process. Lastly, our results have therapeutic implications suggesting that DNMTIs will prevent EMT in cancer cells and subsequently decrease the risk of ovarian cancer metastasis.

Materials and Methods

Cell culture

The ovarian cancer cell lines SKOV3, OV90, OVCAR3, IGROV1, Hey, and HeyC2 were obtained from the American Type Culture Collection (ATCC). IOSE cells are telomerase immortalized surface epithelial ovarian cells and were a gift from Dr. N. Auersperg from University of British Columbia.[49] Cells were maintained in RPMI-1640 (OVCAR3 and IGROV1) or medium containing 1:1 MCDB 105 (Sigma-Aldrich) and M199 (Cellgro) supplemented with 10% fetal bovine serum and 1% penicillin and streptomycin solution. Cells were treated with TGF-β1 (R&D Systems) and/or the hypomethylating agent SGI-110 (Astex Pharmaceuticals) using doses of 5 ng/ml and 5 μM, respectively. Treatment with TGF-β continued for up to 120 h and biological effects were measured up to 48 h after TGF-β removal.

DNA extraction and bisulfite conversion

Genomic DNA was extracted using the QIAamp DNA mini-kit (Qiagen). Genomic DNA was treated with sodium bisulfite using the EZ DNA Methylation-Gold kit (Zymo Research). Bisulfite converted DNA was used to measure DNA methylation.

DNA methylation profiling

Genome-wide DNA methylation profiling used Infinium HumanMethylation450 BeadChip (HM450; Illumina) and was carried out at the University of Chicago Genomics Core, Knapp Center for Biomedical Discovery (Chicago, IL) following procedures provided by Illumina. Data quality and determination of methylation levels of 485,577 CpG sites included in the

HM450 BeadChip were assessed using Illumina GenomeStudio Data Analysis Software. Methylation levels were calculated as β-values ranging from 0 for unmethylated, to 1 for fully methylated CpG sites. Data have been deposited in GEO accession number GSE56621.

DNA methylation analysis by pyrosequencing

Methylation levels of CpG sites in the promoter of selected genes and long interspersed element-1 (LINE-1) were determined by bisulfite pyrosequencing performed at EpigenDx. In brief, target sequences containing CpG methylation sites were amplified by PCR using specific primers. One of the PCR primers was biotinylated to allow for purification of the PCR product using streptavidin sepharose beads (Amersham). Sepharose beads containing the immobilized PCR product were purified, washed, and denatured (0.2 M NaOH) using the Pyrosequencing Vacuum Prep Tool (Qiagen). The pyrosequencing primer (0.2 μM) was annealed to the purified single-stranded PCR product, which was then sequenced using the Pyrosequencing PSQ96 HS System (Qiagen). The methylation level of each locus was determined and expressed as a percentage using QCpG software (Qiagen).

Transfection

Transient knockdown of *p65* (*RELA*) was performed by using small interfering RNA (siRNA) (siGenome SMART pool, Dharmacon) or scrambled siRNA (control, Dharmacon) and the DreamFect Gold transfection reagent (OZ Biosciences).

RNA isolation and RT-PCR

Total RNA was extracted from cultured cells with the RNA Stat-60 reagent (Tel-Test, Inc.). The iScript cDNA Synthesis kit (Bio-Rad) was used for reverse transcription and iTaq SYBR Green Supermix with ROX (Bio-Rad) was used for real-time PCR amplification. Relative changes in gene expression were calculated by the $2^{-\Delta\Delta CT}$ method using GAPDH for normalization. Some transcripts were amplified by semiquantitative RT-PCR using GoTaq Green master mix (Promega). PCR products were resolved by agarose gel electrophoresis and visualized by ethidium bromide staining. Densitometric analysis using the ImageJ software (http://imagej.nih.gov/ij) was used for quantitation of amplicons relative to GAPDH. The sequences of primers and number of cycles of amplification used for PCR are included in **Supplementary Table S2**.

EMT pathway analysis

Expression of 84 genes associated with EMT was analyzed by real-time RT-PCR using RT^2 Profiler PCR arrays. The EMT Profiler arrays, the RT^2 First Strand kit, and the RT^2 SYBR Green ROX qPCR master mix were purchased from SA Bioscience Corporation. Total RNA (500 ng) was reverse transcribed, cleared of DNA contamination, and then amplified using the real-time cycler 7900HT (Applied Biosystems). Relative changes in gene expression were estimated by the $2^{-\Delta\Delta CT}$ method using the average of the 5 housekeeping genes (*ACTB, B2M, GAPDH, HPRT1, RPLPO*) included in the array as reference for normalization, following the protocol provided by the manufacturer.

Nuclear protein extraction and DNMT activity

Nuclear proteins were extracted using the EpiQuik Nuclear Extraction kit (EpigenTek). Total DNMT activity in nuclear extracts was determined using the EpiQuik DNMT Activity/Inhibition Assay Ultra kit (EpigenTek). DNMT 1 activity was calculated as OD/h/mg of protein.

Western blotting

Equal amounts of protein were separated by SDS-PAGE and electroblotted onto polyvinylidene difluoride membranes (Millipore). After blocking, membranes were probed with primary antibodies overnight at 4°C. Antibodies for DNMT-1 (#5032), vimentin (# 3932), and E-Cadherin (#3195), were from Cell Signaling Technology, for DNMT-3B (#ab79822, clone EPR3523) from Abcam Inc., for GAPDH (# H86504M) from Meridian Life Sciences, Inc., and for β-Actin (#A5441, clone AC-15) from Sigma. After incubation with HRP-conjugated secondary antibody, antigen-antibody complexes were visualized using an enhanced chemiluminescence detection system (SuperSignal West Pico, Thermo Scientific). Images were captured by a luminescent image analyzer with a CCD camera (LAS 3000, Fuji Film). Densitometry analysis was performed with ImageJ 1.48 software.

Statistical analysis

Average methylation signals on the CpG sites within each CpG island (CGI) and/or promoter region defined as regions encompassing −2000 to +500 nucleotides relative to the TSS were hierarchically clustered with Pearson dissimilarity and average linkage as clustering parameters. Principal component analysis on the average methylation signals was conducted using Partek Genomics Suite (version 6.5). TGF-β-induced methylation changes were identified in both individual CpG level and in region-specific level by considering all the CpG sites within a CGI and/or promoter region. For individual CpG level, analysis of variance (ANOVA) was used on the logit transformation of the β-values identified in the HM450 BeadChip. This transformation effectively converts the β-value (ranges from 0–1) into a normal-like distribution and has been used previously for differential methylation analysis.[50] For region specific analysis, a generalized linear model was used by treating different CpG sites within a specific region as repeated measures. Such strategy effectively uses all the CpG site signals within the region, and takes into the consideration the consistency of the methylation changes across all the sites. Since increased or decreased methylation levels for the high or low methylated CpG sites (with high or low β-values) cannot be effectively identified, the CpG sites with β-value ≥ 0.9 or ≤ 0.1 in the control condition were not included in the region specific analysis. In order to correct the P-values for the multiple hypothesis testing, false discovery rates (FDR) were calculated by using an improved Benjamini-Hochberg procedure.[51] The CpG sites/CGIs with FDR ≤ 0.05 were considered as significant changes. Lists of differentially

methylated CpG sites genes between groups were imported into Ingenuity Pathway Analysis (IPA Ingenuity Systems) software to identify gene pathways and networks regulated by methylation. For other variables compared among experimental groups, significant differences ($P < 0$ .05) were determined by t-tests.

Disclosure of Potential Conflicts of Interest

No potential conflicts of interest were disclosed.

Acknowledgments

We thank Dr. Mohammad Azab and Pietro Taverna (Astex Pharmaceuticals, Inc.) for providing SGI-110 and helpful scientific comments, and Dr. Pieter Faber of the University of Chicago Genomics Core; Knapp Center for Biomedical Discovery (KCBD) for technical assistance.

Funding

This work was made possible by funding from the Ovarian Cancer Research Fund [PPDIU01.2011] (KN and DM) and US Department of Veterans Affairs to DM.

Supplemental Materials

Supplemental data for this article can be accessed on the publisher's website.

References

1. Jones PA, Baylin SB. The fundamental role of epigenetic events in cancer. Nat Rev Genet 2002; 3:41528; PMID:12042769; http://dx.doi.org/10.1038/nrg962
2. Das PM, Singal R. DNA methylation and cancer. J Clin Oncol 2004; 22:463242; PMID:15542813; http://dx.doi.org/10.1200/JCO.2004.07.151
3. Patra SK, Patra A, Rizzi F, Ghosh TC, Bettuzzi S. Demethylation of (Cytosine-5-C-methyl) DNA and regulation of transcription in the epigenetic pathways of cancer development. Cancer Metast Rev 2008; 27:31534; PMID:18246412; http://dx.doi.org/10.1007/s10555-008-9118-y
4. Zhu JK. Active DNA demethylation mediated by DNA glycosylases. Annu Rev Genet 2009; 43:14366; PMID:19659441; http://dx.doi.org/10.1146/annurev-genet-102108-134205
5. Ito S, D'Alessio AC, Taranova OV, Hong K, Sowers LC, Zhang Y. Role of Tet proteins in 5mC to 5hmC conversion, ES-cell self-renewal and inner cell mass specification. Nature 2010; 466:112933; PMID:20639862; http://dx.doi.org/10.1038/nature09303
6. Thiery JP. Epithelial-mesenchymal transitions in tumour progression. Nat Rev Cancer 2002; 2:44254; PMID:12189386; http://dx.doi.org/10.1038/nrc822
7. Perl AK, Wilgenbus P, Dahl U, Semb H, Christofori G. A causal role for E-cadherin in the transition from adenoma to carcinoma. Nature 1998; 392:1903; PMID:9515965; http://dx.doi.org/10.1038/32433
8. Nagafuchi A, Shirayoshi Y, Okazaki K, Yasuda K, Takeichi M. Transformation of cell adhesion properties by exogenously introduced E-cadherin cDNA. Nature 1987; 329:3413; PMID:3498123; http://dx.doi.org/10.1038/329341a0
9. Moreno-Bueno G, Cubillo E, Sarrio D, Peinado H, Rodriguez-Pinilla SM, Villa S, Bolós V, Jordá M, Fabra A, Portillo F, et al. Genetic profiling of epithelial cells expressing E-cadherin repressors reveals a distinct role for Snail, Slug, and E47 factors in epithelial-mesenchymal transition. Cancer Res 2006; 66:954356; PMID:17018611; http://dx.doi.org/10.1158/0008-5472.CAN-06-0479
10. Lombaerts M, van Wezel T, Philippo K, Dierssen JW, Zimmerman RM, Oosting J, van Eijk R, Eilers PH, van de Water B, Cornelisse CJ, et al. E-cadherin transcriptional downregulation by promoter methylation but not mutation is related to epithelial-to-mesenchymal transition in breast cancer cell lines. Br J Cancer 2006; 94:66171; PMID:16495925
11. Dumont N, Wilson MB, Crawford YG, Reynolds PA, Sigaroudinia M, Tlsty TD. Sustained induction of epithelial to mesenchymal transition activates DNA methylation of genes silenced in basal-like breast cancers. Proc Natl Acad Sci U S A 2008; 105:1486772; PMID:18806226; http://dx.doi.org/10.1073/pnas.0807146105
12. Lin T, Ponn A, Hu X, Law BK, Lu J. Requirement of the histone demethylase LSD1 in Snai1-mediated transcriptional repression during epithelial-mesenchymal transition. Oncogene 2010; 29:4896904; PMID:20562920; http://dx.doi.org/10.1038/onc.2010.234
13. Dong C, Wu Y, Wang Y, Wang C, Kang T, Rychahou PG, Chi YI, Evers BM, Zhou BP. Interaction with Suv39H1 is critical for Snail-mediated E-cadherin repression in breast cancer. Oncogene 2013; 32:135162; PMID:22562246; http://dx.doi.org/10.1038/onc.2012.169
14. Dong C, Wu Y, Yao J, Wang Y, Yu Y, Rychahou PG, Evers BM, Zhou BP. G9a interacts with Snail and is critical for Snail-mediated E-cadherin repression in human breast cancer. J Clin Invest 2012; 122:146986; PMID:22406531; http://dx.doi.org/10.1172/JCI57349
15. Baldwin RL, Tran H, Karlan BY. Loss of c-myc repression coincides with ovarian cancer resistance to transforming growth factor beta growth arrest independent of transforming growth factor betaSmad signaling. Cancer Res 2003; 63:14139; PMID:12649207
16. Dowdy SC, Mariani A, Janknecht R. HER2Neu- and TAK1-mediated up-regulation of the transforming growth factor beta inhibitor Smad7 via the ETS protein ER81. J Biol Chem 2003; 278:4437784; PMID:12947087; http://dx.doi.org/10.1074/jbc.M307202200
17. Cardillo MR, Yap E, Castagna G. Molecular genetic analysis of TGF-beta1 in ovarian neoplasia. J Exp Clin Cancer Res 1997; 16:4956; PMID:9148861
18. Rodriguez GC, Haisley C, Hurteau J, Moser TL, Whitaker R, Bast RC, Jr., Stack MS. Regulation of invasion of epithelial ovarian cancer by transforming growth factor-beta. Gynecol Oncol 2001; 80:24553; PMID:11161867; http://dx.doi.org/10.1006/gyno.2000.6042
19. Wakahara K, Kobayashi H, Yagyu T, Matsuzaki H, Kondo T, Kurita N, Sekino H, Inagaki K, Suzuki M, Kanayama N, et al. Transforming growth factor-beta1-dependent activation of Smad23 and up-regulation of PAI-1 expression is negatively regulated by Src in SKOV-3 human ovarian cancer cells. J Cell Biochem 2004; 93:43753; PMID:15372629; http://dx.doi.org/10.1002/jcb.20160
20. Cao L, Shao M, Schilder J, Guise T, Mohammad KS, Matei D. Tissue transglutaminase links TGF-beta, epithelial to mesenchymal transition and a stem cell phenotype in ovarian cancer. Oncogene 2012; 31:252134; PMID:21963846; http://dx.doi.org/10.1038/onc.2011.429
21. Abendstein B, Stadlmann S, Knabbe C, Buck M, Muller-Holzner E, Zeimet AG, Marth C, Obrist P, Krugmann J, Offner FA. Regulation of transforming growth factor-beta secretion by human peritoneal mesothelial and ovarian carcinoma cells. Cytokine 2000; 12:11159; PMID:10880260; http://dx.doi.org/10.1006/cyto.1999.0632
22. Bartlett JM, Langdon SP, Scott WN, Love SB, Miller EP, Katsaros D, Smyth JF, Miller WR. Transforming growth factor-beta isoform expression in human ovarian tumours. Eur J Cancer 1997; 33:2397403; PMID:9616289; http://dx.doi.org/10.1016/S0959-8049(97)00304-3
23. Bristow RE, Baldwin RL, Yamada SD, Korc M, Karlan BY. Altered expression of transforming growth factor-beta ligands and receptors in primary and recurrent ovarian carcinoma. Cancer 1999; 85:65868; PMID:10091739; http://dx.doi.org/10.1002/(SICI)1097-0142(19990201)85:3%3c658::AID-CNCR16%3e3.0.CO;2-M
24. Massague J. TGFbeta signaling: receptors, transducers, and Mad proteins. Cell 1996; 85:94750; PMID:8674122; http://dx.doi.org/10.1016/S0092-8674(00)81296-9
25. Chen T, Triplett J, Dehner B, Hurst B, Colligan B, Pemberton J, Graff JR, Carter JH. Transforming growth factor-beta receptor type I gene is frequently mutated in ovarian carcinomas. Cancer Res 2001; 61:467982; PMID:11406536
26. Lynch MA, Nakashima R, Song H, DeGroff VL, Wang D, Enomoto T, Weghorst CM. Mutational analysis of the transforming growth factor beta receptor type II gene in human ovarian carcinoma. Cancer Res 1998; 58:422732; PMID:9766642
27. Yang AS, Estecio MR, Doshi K, Kondo Y, Tajara EH, Issa JP. A simple method for estimating global DNA methylation using bisulfite PCR of repetitive DNA elements. Nucleic Acids Res 2004; 32:e38; PMID:14973332; http://dx.doi.org/10.1093/nar/gnh032
28. Weisenberger DJ, Campan M, Long TI, Kim M, Woods C, Fiala E, Ehrlich M, Laird PW. Analysis of repetitive element DNA methylation by MethyLight. Nucleic Acids Res 2005; 33:682336; PMID:16326863; http://dx.doi.org/10.1093/nar/gki987
29. Yang AS, Doshi KD, Choi SW, Mason JB, Mannari RK, Gharybian V, Luna R, Rashid A, Shen L, Estecio MR, et al. DNA methylation changes after 5-aza-2'-deoxycytidine therapy in patients with leukemia. Cancer Res 2006; 66:5495503; PMID:16707479; http://dx.doi.org/10.1158/0008-5472.CAN-05-2385
30. Tahiliani M, Koh KP, Shen Y, Pastor WA, Bandukwala H, Brudno Y, Agarwal S, Iyer LM, Liu DR, Aravind L, et al. Conversion of 5-methylcytosine to 5-hydroxymethylcytosine in mammalian DNA by MLL partner TET1. Science 2009; 324:9305; PMID:19372391; http://dx.doi.org/10.1126/science.1170116
31. Papageorgis P, Lambert AW, Ozturk S, Gao F, Pan H, Manne U, Alekseyev YO, Thiagalingam A, Abdolmaleky HM, Lenburg M, et al. Smad signaling is required to maintain epigenetic silencing during breast cancer progression. Cancer Res 2010; 70:96878; PMID:20086175; http://dx.doi.org/10.1158/0008-5472.CAN-09-1872
32. Foulks JM, Parnell KM, Nix RN, Chau S, Swierczek K, Saunders M, Wright K, Hendrickson TF, Ho KK, McCullar MV, et al. Epigenetic drug discovery: targeting DNA methyltransferases. J Biomol Screen 2012; 17:217; PMID:21965114; http://dx.doi.org/10.1177/1087057111421212

33. Tellez CS, Grimes MJ, Picchi MA, Liu Y, March TH, Reed MD, Oganesian A, Taverna P, Belinsky SA. SGI-110 and entinostat therapy reduces lung tumor burden and reprograms the epigenome. Int J Cancer J 2014; PMID:24668305
34. Beauchef G, Bigot N, Kypriotou M, Renard E, Poree B, Widom R, Dompmartin-Blanchere A, Oddos T, Maquart FX, Demoor Mk, et al. The p65 subunit of NF-kappaB inhibits COL1A1 gene transcription in human dermal and scleroderma fibroblasts through its recruitment on promoter by protein interaction with transcriptional activators (c-Krox, Sp1, and Sp3). J Biol Chem 2012; 287:346278; PMID:22139845; http://dx.doi.org/10.1074/jbc.M111.286443
35. Kalluri R, Weinberg RA. The basics of epithelial-mesenchymal transition. J Clin Invest 2009; 119:14208; PMID:19487818; http://dx.doi.org/10.1172/JCI39104
36. Mani SA, Guo W, Liao MJ, Eaton EN, Ayyanan A, Zhou AY, Brooks M, Reinhard F, Zhang CC, Shipitsin M, et al. The epithelial-mesenchymal transition generates cells with properties of stem cells. Cell 2008; 133:70415; PMID:18485877; http://dx.doi.org/10.1016/j.cell.2008.03.027
37. Cao Q, Yu J, Dhanasekaran SM, Kim JH, Mani RS, Tomlins SA, Mehra R, Laxman B, Cao X, Yu J, et al. Repression of E-cadherin by the polycomb group protein EZH2 in cancer. Oncogene 2008; 27:727484; PMID:18806826; http://dx.doi.org/10.1038/onc.2008.333
38. Herranz N, Pasini D, Diaz VM, Franci C, Gutierrez A, Dave N, Escrivà M, Hernandez-Muñoz I, Di Croce L, Helin K, et al. Polycomb complex 2 is required for E-cadherin repression by the Snail1 transcription factor. Mol Cell Biol 2008; 28:477281; PMID:18519590; http://dx.doi.org/10.1128/MCB.00323-08
39. Chaffer CL, Marjanovic ND, Lee T, Bell G, Kleer CG, Reinhardt F, D'Alessio AC, Young RA, Weinberg RA. Poised chromatin at the ZEB1 promoter enables breast cancer cell plasticity and enhances tumorigenicity. Cell 2013; 154:6174; PMID:23827675; http://dx.doi.org/10.1016/j.cell.2013.06.005
40. O'Hagan HM, Mohammad HP, Baylin SB. Double strand breaks can initiate gene silencing and SIRT1-dependent onset of DNA methylation in an exogenous promoter CpG island. PLoS Genet 2008; 4:e1000155; http://dx.doi.org/10.1371/journal.pgen.1000155
41. O'Hagan HM, Wang W, Sen S, Destefano Shields C, Lee SS, Zhang YW, Clements EG, Cai Y, Van Neste L, Easwaran H, et al. Oxidative damage targets complexes containing DNA methyltransferases, SIRT1, and polycomb members to promoter CpG Islands. Cancer Cell 2011; 20:60619; PMID:22094255; http://dx.doi.org/10.1016/j.ccr.2011.09.012
42. Roll JD, Rivenbark AG, Sandhu R, Parker JS, Jones WD, Carey LA, Livasy CA, Coleman WB. Dysregulation of the epigenome in triple-negative breast cancers: basal-like and claudin-low breast cancers express aberrant DNA hypermethylation. Exp Mol Pathol 2013; 95:27687; PMID:24045095; http://dx.doi.org/10.1016/j.yexmp.2013.09.001
43. Zeng Q, Li W, Lu D, Wu Z, Duan H, Luo Y, Feng J, Yang D, Fu L, Yan X. CD146, an epithelial-mesenchymal transition inducer, is associated with triple-negative breast cancer. Proc Natl Acad Sci U S A 2012; 109:112732; PMID:22210108; http://dx.doi.org/10.1073/pnas.1111053108
44. Malouf GG, Taube JH, Lu Y, Roysarkar T, Panjarian S, Estecio MR, Jelinek J, Yamazaki J, Raynal NJ, Long H. Architecture of epigenetic reprogramming following Twist1-mediated epithelial-mesenchymal transition. Genome Biol 2013; 14:R144; PMID:24367927; http://dx.doi.org/10.1186/gb-2013-14-12-r144
45. Fang F, Zuo Q, Pilrose J, Wang Y, Shen C, Li M, Wulfridge P, Matei D, Nephew KP. Decitabine reactivated pathways in platinum resistant ovarian cancer. Oncotarget 2014; 5:357989; PMID:25003579
46. Matei D, Fang F, Shen C, Schilder J, Arnold A, Zeng Y, Berry WA, Huang T, Nephew KP, et al. Epigenetic resensitization to platinum in ovarian cancer. Cancer Res 2012; 72:2197205; PMID:22549947; http://dx.doi.org/10.1158/0008-5472.CAN-11-3909
47. Tsai HC, Li H, Van Neste L, Cai Y, Robert C, Rassool FV, Shin JJ, Harbom KM, Beaty R, Pappou E. Transient low doses of DNA-demethylating agents exert durable antitumor effects on hematological and epithelial tumor cells. Cancer Cell 2012; 21:43046; PMID:22439938; http://dx.doi.org/10.1016/j.ccr.2011.12.029
48. Naeem H, Wong NC, Chatterton Z, Hong MK, Pedersen JS, Corcoran NM, Hovens CM, Macintyre G. Reducing the risk of false discovery enabling identification of biologically significant genome-wide methylation status using the HumanMethylation450 array. BMC Genomics 2014; 15:51; PMID:24447442; http://dx.doi.org/10.1186/1471-2164-15-51
49. Auersperg N, Wong AS, Choi KC, Kang SK, Leung PC. Ovarian surface epithelium: biology, endocrinology, and pathology. Endocr Rev 2001; 22:25588; PMID:11294827
50. Du P, Zhang X, Huang CC, Jafari N, Kibbe WA, Hou L, Lin SM. Comparison of Beta-value and M-value methods for quantifying methylation levels by microarray analysis. BMC Bioinformatics 2010; 11:587; PMID:21118553; http://dx.doi.org/10.1186/1471-2105-11-587
51. Benjamini Y, Yekutieli, D. The control of the false discovery rate in multiple testing under dependency Ann Stat 2001; 29:116588; http://dx.doi.org/10.1214/aos/1013699998